厚生労働科学研究費補助金（医療機器開発推進研究事業）
分担研究報告書

ＤＤＳ用微細球殻気泡の基本物理特性と気泡分散液での超音波減衰に関する研究

研究分担者　藤川　重雄　北海道大学大学院工学研究科教授

研究要旨：次世代の投薬形態として、DDS(Drug Delivery System)に気泡を利用した技術が期待されている。本研究は、DDS 技術実現のための基礎研究として、水中における殻付微細気泡に周波数の異なる超音波を照射し、気泡の共振による超音波の吸収を解析することで、殻付微細気泡の共振周波数を特定することを目的としてなされたものである。この目的達成のために、殻付微細気泡の形状，径分布等の基本物理特性を明らかにするとともに、これらの特性と吸収との関係を明らかにした。

A. 研究目的

本研究は、DDS 技術実現のための基礎研究として、水中における殻付微細気泡に周波数の異なる超音波を照射し、共振による超音波の吸収を解析することで、殻付微細気泡の共振周波数を特定することを目的としてなされたものである。

B. 研究方法

リン脂質膜からなる球状の殻を持ち、内部が液体で満たされたリポソームの粒径は数μm から数十 nm まで広く存在している。実験は、超音波ホモジナイザーによりリポソームの粒径の整え、その内部の液体を C_3F_8 ガスで置換したものを殻付微細気泡として使用した。殻付微細気泡の形状は、走査電子顕微鏡像で観察した。殻付微細気泡を含んだ懸濁液を希釈し、異なる濃度での超音波照射の実験を行った。（倫理面への配慮）殻付微細気泡の基礎物理特性に関する実験であるため、特別な配慮はしなかった。

C. 研究結果

図 1 は 1～2MHz 及び 10MHz 付近において大きな超音波の音響減衰が見受けられ、ピークが２つ存在していることがわかる。粒径分布の測定結果から、実験で用いた試料は 200nm、1000nm 付近を中心とした２つの粒径を持っていた。超音波減衰図と粒径分布図の２つの異なる測定方法により得られた結果が、同一の推察を導くことより、本実験では２つの粒径分布を持つ殻付微細気泡によって、２つの超音波減衰のピークが現れたものではないかと考える。

電子顕微鏡による観察によって初めて得られた写真はこの仮説を支えるものである。

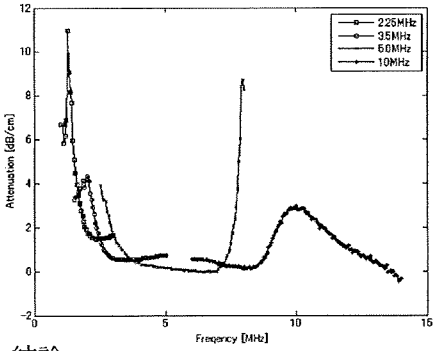

D. 結論

本研究では、ナノスケールの殻付微細気泡を通過した超音波は特定の周波数において減衰を伴うことを明らかにした。

E. 研究発表

学会発表（計４件）

(1) 金川哲也・矢野　猛・渡部正夫・藤川重雄，殻付き微細気泡群を含む液体中における非線形波の伝播，日本流体力学会年会講演論文集(CD-ROM),pp.1-4,2008.

(2) Imai, R., Nakagawa, T., Kanagawa, T., Watanabe, M., Fujikawa, S., Acoustic Characteristics of Ultrasound in Water Containing Lipid Microbubbles, ExHFT-7, June 28-July 3, 2009, Krakow, Poland, (Accepted for presentation). 他２編省略.

研究成果の刊行に関する一覧表

別紙

研究成果の刊行に関する一覧表

雑誌

発表者氏名	論文タイトル名	発表誌名	巻号	ページ	出版年
Chen S, Ndhlovu LC, Takahashi T, Takeda K, Ikarashi Y, Kikuchi T, Murata K, Pandolfi PP, Riccardi C, Ono M, Sugamura K, Ishii N	Co-inhibitory roles for glucocorticoid-induced TNF receptor in CD1d-dependent natural killer T cells.	*Eur J Immunol*	38 (8)	2229-2240	2008
Furukawa H, Kitazawa H, Kaneko I, Matsubara M, Nose M, Ono M	Role of 2B4-mediated signals in the pathogenesis of a murine hepatitis model independent of Fas and Valpha14 NKT cells	*Immunology*	128	151-158	2008
Huan Z, Nakayama K, Nakayama N, Ishibashi M, Yeasmin S, Katagiri A, Purwana IN, Iida K, Maruyama R, Fukumoto M, Miyazaki K:	Genetic classification of ovarian carcinoma based on microsatellite analysis: relationship to clinicopathological features and patient survival.	Oncol Rep	19(3)	775-781	2008
Imai, R., Nakagawa, T., Kanagawa, T., Watanabe, M., Fujikawa, S.	Acoustic Characteristics of Ultrasound in Water Con-taining Lipid Microbubbles	ExHFT-7 Krakow, Poland			2009

Ishibashi M, Nakayama K, Yeasmin S, Katagiri A, Iida K, Nakayama N, Fukumoto M, Miyazaki K	A BTB/POZ gene, NAC-1, a tumor recurrence-associated gene, as a potential target for Taxol resistance in ovarian cancer.	Clin Cancer Res	14(10)	3149-3155	2008
金川哲也・矢野猛・渡部正夫・藤川重雄	殻付き微細気泡群を含む液体中における非線形波の伝播	日本流体力学会年会講演論文集		(CD-ROM), pp. 1-4,	2008
Kaneko I, Hishinuma T, Suzuki K, Owada Y, Kitanaka N, Kondo H, Goto J, Furukawa H, Ono M.	Prostaglandin F(2alpha) regulates cytokine responses of mast cells through the receptors for prostaglandin E	*Biochem Biophys Res Commun*	367	590-6	2008
Kashino G, Kondoh T, Nariyama N, Umetani K, Ohigashi T, Shinohara K, Kurihara A, Fukumoto M, Tanaka H, Maruhashi A, Suzuki M, Kinashi Y, Yong L, Masunaga S, Watanabe M, Ono K	Inductions of DNA double strand breaks and cellular migrations through the bystander effects in the cells irradiated with slit type microplanar beam of the SPring-8 synchrotron.	Int J Radiat Oncol Biol Physic	74 (1)	119-36	2009
Kodama T, Tomita Y, Watanabe Y, Koshiyama K, Yano T, Fujikawa S.	Cavitation bubbles mediated molecular delivery during sonoporation.	Journal of Biomechanical Science and Engineering	4	124-140	2009

Koshiyama K, Kodama T, Yano T, Fujikawa S.	Molecular dynamics simulation of structural changes of lipid bilayers induced by shock waves: effects of incident angles.	Biochimica et Biophysica Acta (BBA) - Biomembranes.	1778(6)	1423-1428	2008
Kuroda JI, Kuratsu JI, Yasunaga M, Koga Y, Saito Y, Matsumura Y.	Potent antitumor effect of SN-38-incorporating polymeric micelle, NK012, against malignant glioma.	Int J Cancer	124 (11)	2505-2511	2008
Kuwahara Y, Li L, Baba T, Nakagawa H, Shimura T, Yamamoto Y, Ohkubo Y, Fukumoto M.	Clinically relevant radioresistant cells efficiently repair DNA double-strand breaks induced by X-rays.	Cancer Sci.	100 (4)	747-752	2009
Li L, Shoji W, Ohshima H, Obinata M, Fukumoto M, Kanno N	Crucial role of peroxiredoxin III in placental antioxidant defense of mice.	FEBS Lett	582(16)	2431-2434	2008
Matsumura Y.	Polymeric micellar delivery systems in oncology.	Jpn J Clin Oncol	38	793-802	2008
Matsumura Y.	Poly (amino acid) micelle nanocarriers in preclinical and clinical studies.	Adv Drug Deliv Rev	60	899-914	2008
Miyashita H, Mori S, Fukumoto Y, Sato A, Fukumoto M, Kawamura H:	Loss of heterozygosity of the PTH/PTHrP type 1 recptor in oral squamous cell carcinoma.	Mol Med Report	1	821-825	2008

Mori S, Tanda N, Ito MR, Oishi H, Tsubaki T, Komori H, Zhang MC, Ono M, Nishimura M, Nose M.	Novel recombinant congenic mouse strain developing arthritis with enthesopathy.	*Pathol Int*	58	407-14	2008
Nakajima TE, Yanagihara K, Takigahira M, et al.	Antitumor effect of SN-38-releasing polymeric micelles, NK012, on spontaneous peritoneal metastases from orthotopic gastric cancer in mice compared with irinotecan.	Cancer Res	68	9318-22	2008
Nakajima TE, Yasunaga M, Kano Y, et al.	Synergistic antitumor activity of the novel SN-38-incorporating polymeric micelles, NK012, combined with 5-fluorouracil in a mouse model of colorectal cancer, as compared with that of irinotecan plus 5-fluorouracil.	Int J Cancer	122	2148-53	2008
Nakayama N, Nakayama K, Yeasmin S, Ishibashi M, Katagiri A, Iida K, Fukumoto M, Miyazaki K.	KRAS or BRAF mutation status is a useful predictor of sensitivity to MEK inhibition in ovarian cancer	Br J Cancer	99(12)	2020-2028	2008

Nariyama N, Ohhigashi T, Umetani K, Shinohara K, Tanaka H, Maruhashi A, Kashino G, Kurihara A, Kondo T, Fukumoto M:	Spectromicoscopic film dosimetry for high-energy microbeam from synchrotron radiation.	Appl Rad Isot	67(1)	155-9.	2009
Ohtake Y, Maruko A, Kuwahara Y, Fukumoto M, Ohkubo Y.	Stabilities of 67ga- and 111In-labeled transferrin in vitro.	Protein Pept Lett.	16(2)	138-42,	2009
Ohtake Y., Maruko A., Ohishi N., Fukumoto M, Ohkubo Y	Effect of aging on EGF-induced proliferative response in primary cultured periportal and perivenous hepatocytes.	J Hepatol,	48(2):	246-54	2008.
Roudkenar MH, Halabian R, Ghasemipour Z, Roushandeh AM, Rouhbakhsh M, Nekogoftar M, Kuwahara Y, Fukumoto M, Shokrgozar MA.	Neutrophil gelatinase-associated lipocalin acts as a protective factor against H(2)O(2) toxicity.	Arch Med Res	39(6)	560-566	2008

Roudkenar MH, Li L, Baba T, Kuwahara Y, Nakagawa H, Wang L, Kasaoka S, Ohkubo Y, Ono K, Fukumoto M:	Gene expression profiles in mouse liver cells after exposure to different types of radiation.	J Radiat Res	49(1)	29-40	2008.
Saito Y, Yasunaga M, Kuroda J, Koga Y, Matsumura Y.	Enhanced distribution of NK012, a polymeric micelle-encapsulated SN-38, and sustained release of SN-38 within tumors can beat a hypovascular tumor.	Cancer Sci	99	1258-64.	2008
Sumitomo M, Koizumi F, Asano T, et al.	Novel SN-38-incorporated polymeric micelle, NK012, strongly suppresses renal cancer progression.	Cancer Res	68	1631-5	2008
Suzuki R, Oda Y, Utoguchi N, Namai E, Taira Y, Okada N, Kadowaki N, Kodama T, Tachibana K, Maruyama K.	A novel strategy utilizing ultrasound for antigen delivery in dendritic cell-based cancer immunotherapy.	Journal of Controlled Release.	133	198-205	2009
Suzuki R, Takizawa T, Negishi Y, et al	Tumor specific ultrasound enhanced gene transfer in vivo with novel liposomal bubbles.	J Control Release	125	137-44	2008
Takeyama J, Sasano H, Fukumoto M:	Giant chordoma occupying the whole abdominal cavity.	Pathology	40(3):	313-314	2008.
Tamai K, Toyoshima M, Tanaka N, Yamamoto N, Owada Y, Kiyonari H, Murata K, Ueno Y, Ono M, Shimosegawa T, Yaegashi N, Watanabe M, Sugamura K.	Loss of hrs in the central nervous system causes accumulation of ubiquitinated proteins and neurodegeneration.	*Am J Pathol.*	173(6)	1806-17	2008

Umemura A, Itoh Y, Itoh K, Yamaguchi K, Nakajima T, Higashitsuji H, Onoue H, Fukumoto M, Okanoue, Fujita J:	Association of gankyrin protein expression with early clinical stages and IGFBP-5 expression in human hepatocellular carcinoma.	Hepatol	47(2):	493-502,	2008.
Watanabe Y, Aoi A, Horie S, Tomita N, Mori S, Morikawa H, Matsumura Y, Vassaux G, Kodama T.	Low-intensity ultrasound and microbubbles enhance the antitumor effect of cisplatin.	Cancer Science.	99(12)	2525-2531	2008
Yamamoto N, Kaneko I, Motohashi K, Sakagami H, Adachi Y, Tokuda N, Sawada T, Furukawa H, Ueyama Y, Fukunaga K, Ono M, Kondo H, Owada Y.	Fatty acid-binding protein regulates LPS-induced TNF-alpha production in mast cells.	*Prostaglandins Leukot Essent Fatty Acids*	79	21-6	2008
Yamashita M, Iwama N, Date F, Chiba R, Ebina M, Miki H, Yamauchi K, Sawai T, Nose M, Sato S, Takahashi T, Ono M.	Characterization of lymphangiogenesis in various stages of idiopathic diffuse alveolar damage.	*Hum Pathol*	40 (4)	542-551	2009
Zhang MC, Furukawa H, Tokunaka K, Saiga K, Date F, Owada Y, Nose M, Ono M.	Mast cell hyperplasia in the skin of Dsg4-deficient hypotrichosis mice, which are long-living mutants of lupus-prone mice.	*Immunogenetics*	60	599-607	2008

研究成果の刊行物・別刷

European Journal of Immunology

Co-inhibitory roles for glucocorticoid-induced TNF receptor in CD1d-dependent natural killer T cells

Shuming Chen[1], Lishomwa C. Ndhlovu[*1], Takeshi Takahashi[1], Kazuyoshi Takeda[2], Yoshinori Ikarashi[3], Toshiaki Kikuchi[4], Kazuko Murata[1], Pier Paolo Pandolfi[5], Carlo Riccardi[6], Masao Ono[7], Kazuo Sugamura[1] and Naoto Ishii[1]*

[1] Department of Microbiology and Immunology, Tohoku University Graduate School of Medicine, Sendai, Japan
[2] Department of Immunology, Juntendo University School of Medicine, Tokyo, Japan
[3] Chemotherapy Division, National Cancer Center Research Institute, Tokyo, Japan
[4] Department of Respiratory Oncology and Molecular Medicine, Institute of Development, Aging and Cancer, Tohoku University, Sendai, Japan
[5] Cancer Biology and Genetics Program, Sloan-Kettering Institute, Memorial Sloan-Kettering Cancer Center, New York, NY, USA
[6] Department of Clinical and Experimental Medicine, Pharmacology Section, Perugia University Medical School, Perugia, Italy
[7] Department of Histopathology, Tohoku University Graduate School of Medicine, Sendai, Japan

Invariant natural killer T (iNKT) cells are a special subset of αβ T cells with invariant TCR, which recognize α-galactosylceramide (α-GalCer) presented by CD1d. In addition to signals through the invariant TCR upon stimulation with α-GalCer, costimulatory signals, such as signals through CD28 and OX40, are indispensable for full activation of iNKT cells. In this study, we investigated the functions of a well-known costimulatory molecule, glucocorticoid-induced TNF receptor (GITR), on Ag-induced iNKT cell activation. Unexpectedly, engagement of GITR by agonistic mAb DTA-1 suppressed proliferation and cytokine production of iNKT cells upon α-GalCer stimulation. In addition, GITR signals in iNKT cells during only the Ag-priming phase was sufficient to inhibit the iNKT cell activation. Consistent with these results, the GITR-deficient iNKT cells showed enhanced proliferation and increased cytokine production upon α-GalCer stimulation both *in vitro* and *in vivo*. Furthermore, the *in vivo* administration of α-GalCer suppressed tumor metastasis more efficiently in GITR-deficient mice than in wild-type mice. Collectively, GITR plays a co-inhibitory role in Ag-induced iNKT cell activation.

Key words: Co-inhibitory signal · Glucocorticoid-induced TNF receptor · Invariant NKT cell

Introduction

CD1d-dependent natural killer T (NKT) cells are a unique subset of αβ T cells that have a Vα14-Jα18 rearrangement in mice and Vα24-Jα18 rearrangement in humans. The invariant TCR specifically recognize a glycosphingolipid, α-galactosylceramide (α-GalCer) presented by an MHC class I-like molecule, CD1d [1]. Once the invariant NKT (iNKT) cells have finished their development in the thymus, they migrate to the periphery, and are primarily maintained in the spleen, liver, and bone marrow [2]. Upon stimulation with the iNKT-specific Ag, α-GalCer, iNKT cells rapidly secrete large amount of various cytokines; they also expand and acquire cytotoxic activity. Accumulating evidence has shown that

Correspondence: Dr. Naoto Ishii
e-mail: ishiin@mail.tains.tohoku.ac.jp

the cytokines secreted by iNKT cells regulate several types of immune responses, including tumor surveillance, autoimmunity, host defense, and immunological tolerance, by modulating the functions of other immune cells [3].

T cell costimulatory molecules, such as the CD28 family and TNF receptor superfamily members, play critical roles in T cell responses. Among them, glucocorticoid-induced TNF receptor (GITR) seems unique for its bidirectional effects on T cell and NK cell activation. GITR was initially identified as a costimulatory molecule for T cell activation [4], and the agonistic anti-GITR mAb, DTA-1, enhances T cell responses in several disease models, such as tumor rejection, autoimmune reaction, GVH disease, and viral infection [5–7]. However, several observations have shown that GITR signals can serve as an inhibitory factor in T cell responses. Ronchetti *et al.* [8] demonstrated that GITR-deficient T cells show higher proliferative responses and enhanced IL-2 production upon stimulation with anti-CD3 mAb, as compared with wild-type (WT) T cells. In contrast, the full stimulation of both TCR and GITR suppresses the Ag-specific proliferation of naïve $CD4^+$ T cells [9]. A previous report also demonstrated that the allogeneic function of conventional $CD4^+$ T cells is impaired by deliberate GITR stimulation [10]. Regarding GITR function on NK cells, a suppressive effect of GITR on NK cells in a culture with GITRL-expressing tumor cells [11] or agonistic anti-GITR mAb [12] has been reported, although a previous paper demonstrated that GITR signals significantly enhanced NK cell activity when GITRL-expressing DC were co-cultured [13]. Furthermore, a recent report has demonstrated that GITRL signals in DC provided by GITR expressed by T cells negatively regulate T cell-mediated allergic inflammation [14]. Thus, the precise roles for the GITR-GITRL interaction on immune responses are still controversial.

With regard to costimulatory signals in NKT cell functions, costimulatory molecules including CD28, ICOS, CD40, and 4–1BB have been demonstrated to promote the Ag-induced activation and cytokine production of NKT cells [15–21]. We have also reported that signals through OX40, a well-known T cell costimulatory molecule, are essential for optimal activation of iNKT cells [22]. Thus, most T cell costimulatory molecules appeared to positively regulate NKT cell function. In addition, a recent report demonstrated that engagement of GITR, which most closely resembles OX40 in their protein and gene structures, on a DN32.D3 NKT hybridoma cell and $NK1.1^+TCR^+$ NKT cells significantly enhanced their functions [23]. However, NK1.1 and TCR co-expression may be an imprecise and potentially misleading criterion for defining NKT cells [3, 24], because $V\alpha14^+$ iNKT cells do not express NK1.1 in some cases, and because some CD1d-independent T cells (a part of $CD8^+$ T cells) also express NK1.1 [3, 24]. Therefore, the functions of GITR in CD1d-dependent iNKT cells are still unclear. To address the GITR role in iNKT cells, we carried out a series of experiments using GITR-deficient (GITR-KO) mice and CD1d tetramers loaded with α-GalCer (α-GalCer/CD1d-tetramer), use of which is one of the most reliable ways to identify iNKT cells. Interestingly, the present results demonstrate that GITR signals negatively regulate the Ag-induced activation of α-GalCer/CD1d-tetramer$^+$ iNKT cells, suggesting that GITR has a co-inhibitory role in iNKT cells.

Results

Expression of GITR on iNKT cells

We first examined the GITR expression on iNKT cells in the thymus, spleen, and liver of WT mice. As shown in Fig. 1A, a similar level of GITR on the iNKT cells in these tissues was observed. Next, GITR expression during Ag-induced activation of α-GalCer/CD1d-tetramer$^+$ iNKT cells was examined. However, to define iNKT cells only at 24 h after Ag stimulation, intracellular staining of TCR Vβ2/7/8, instead of the use of α-GalCer/CD1d-tetramer, was used because surface TCR transiently disappear around 24 h after Ag stimulation [21, 25, 26]. GITR expression on iNKT cells was significantly enhanced during both *in vivo* and *in vitro* activation, and reached the maximum at 72 h (Fig. 1B). The increased expression of GITR upon Ag stimulation indicates that expression profiles of GITR seem to be different from those of other costimulatory molecules and NK cell receptors, which are immediately down-regulated after Ag stimulation [21, 25, 26]. We thus examined the expression of CD28, CD94, NKG2A, ICOS, and OX40 as compared to GITR expression on hepatic iNKT cells 1 day after *in vivo* and *in vitro* stimulation with α-GalCer. Consistent with previous reports, expression of CD28, CD94, NKG2A, and ICOS was remarkably down-regulated, and OX40 remained at a low level while GITR expression was up-regulated (Fig. 1C). To confirm that the activated iNKT cell that lost the surface expression of TCR and other molecules expresses GITR, the cells negative for CD3, NK1.1, CD28, CD94, NKG2A, and CD19 were stained with anti-GITR mAb at 24 h after *in vivo* stimulation with α-GalCer. The frequency of the $CD3^-NK1.1^-CD28^-NKG2A^-CD19^-$ cell population, which contains recently activated iNKT cells, in the mononuclear cells (MNC) of the liver was increased upon Ag stimulation. The ratio of $GITR^+$ cells in this population was also elevated (Fig. 1D). These results indicate that recently activated iNKT cells express GITR in spite of the down-regulation of surface expression of TCR and other costimulatory molecules.

Engagement of GITR by DTA-1 mAb inhibits α-GalCer-induced activation of iNKT cells

The significant expression of GITR on activated iNKT cells (Fig. 1) facilitated examining whether GITR signals may affect iNKT cell function upon Ag stimulation. One previous report regarding GITR role in $CD4^+$ T cells showed that GITR ligation by recombinant mGITRL promoted proliferation of naïve $CD4^+$ T cells upon stimulation with lower dose of Ag, while reducing the proliferation when high-dose Ag was used [9]. We thus investigated the role of GITR signals on iNKT cell activation in the presence of different doses of Ag. Hepatic and splenic MNC were *in vitro* stimulated with higher (100 ng/mL) and lower (2 ng/mL) doses of α-GalCer in the

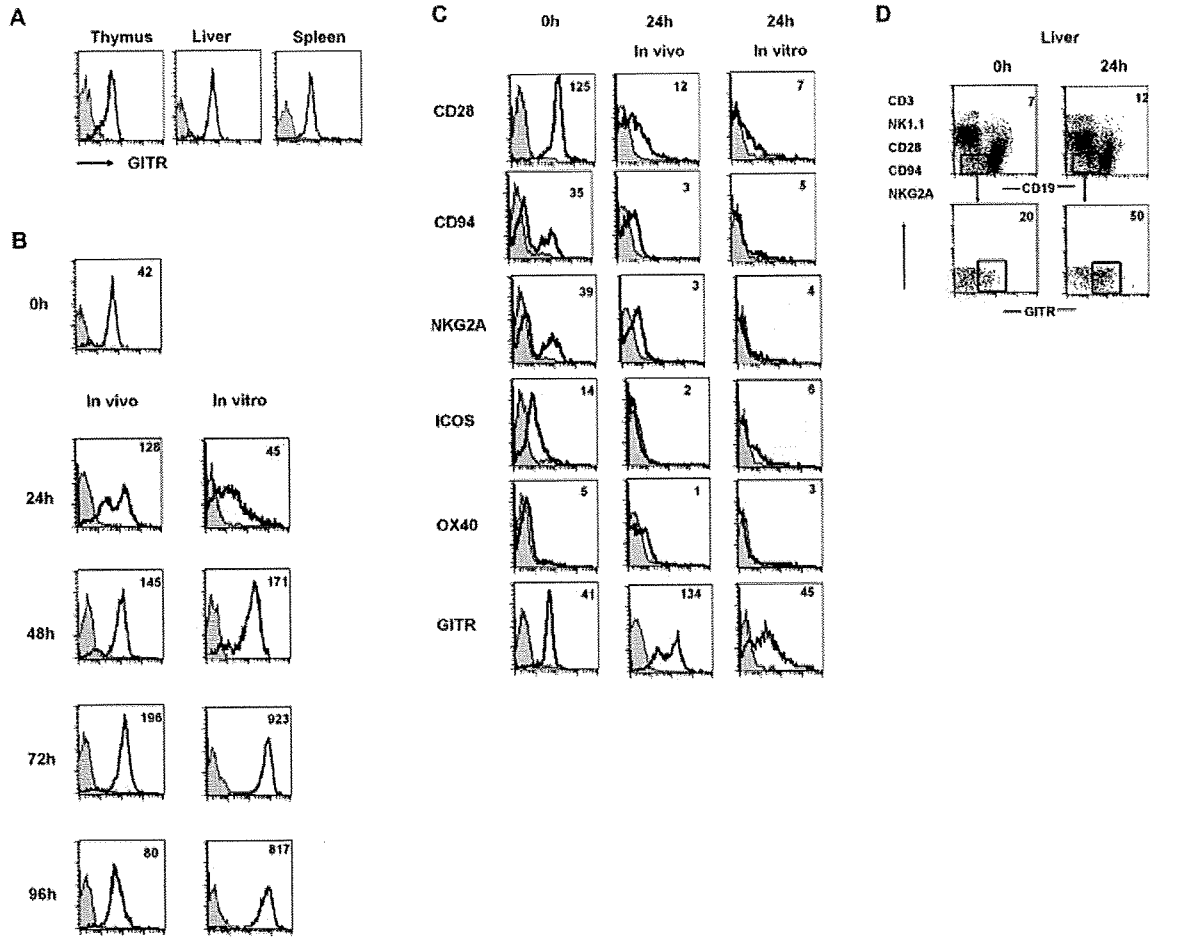

Figure 1. Surface expression of GITR on iNKT cells. (A) MNC from the thymus, liver, and spleen of WT C57BL/6 mice were stained with FITC-TCRβ, PE-conjugated α-GalCer/CD1d-tetramer, and allophycocyanin-conjugated anti-GITR mAb. GITR expression on TCRβ$^+$ α-GalCer/CD1d-tetramer$^+$ iNKT cells is demonstrated as a solid line. The filled gray histogram represents a background staining with allophycocyanin-conjugated control Ab. (B) Surface expression of GITR on electronically gated α-GalCer /CD1d-tetramer$^+$ hepatic iNKT cells was analyzed at 0, 48, 72, and 96 h after α-GalCer stimulation. At 24 h after stimulation, GITR expression on intracellular TCR Vβ2/7/8$^+$ cells was analyzed. Left panels: Mice were injected with 2 μg α-GalCer. Right panels: Hepatic MNC were stimulated with 2 ng/mL α-GalCer. Solid line and filled gray histogram represent a GITR-specific staining and background staining, respectively. The number shown in each panel represents the mean fluorescence intensity for the GITR staining. Similar results were obtained in three independent experiments. (C) Surface expression of the indicated molecules on electronically gated intracellular-TCR Vβ2/7/8$^+$ hepatic iNKT cells were examined 24 h after α-GalCer stimulation *in vivo* (middle panels) and *in vitro* (right panels). The filled gray histograms represent the background staining of isotype-matched control mAb, and the solid lines indicate the staining with the specific mAb for the indicated molecules. The number shown in each panel represents the mean fluorescence intensity of the specific mAb staining. Similar results were obtained in three independent experiments. (D) WT mice were injected with α-GalCer (2 μg/mouse). After 24 h, MNC were isolated from the liver and incubated with CD19-FITC, anti-GITR-allophycocyanin, and biotin-conjugated CD3, NK1.1, CD28, CD94, and NKG2A mAb followed by streptavidin-PE. The upper panels show FITC (horizontal) and PE (vertical) staining of hepatic MNC. The lower panels show GITR expression on electronically gated CD3$^-$NK1.1$^-$CD28$^-$NKG2A$^-$CD19$^-$ cells in the hepatic MNC. The number shown in each panel represents the frequency of the cells in the boxed region. Similar results were obtained in three independent experiments.

presence or absence of the agonistic anti-GITR mAb, DTA-1 [27]. The frequency and the absolute number of α-GalCer/CD1d-tetramer$^+$ TCRβ$^+$ iNKT cells were evaluated on day 4. As shown in Fig. 2A and B, at either concentration, DTA-1 significantly inhibited α-GalCer-induced proliferation of iNKT cells from these tissues. To exclude the possibility that anti-GITR mAb may affect the function of the other GITR-expressing cells, such as T cells, when using MNC, purified iNKT cells were stimulated in the presence of GITR-KO DC, which cannot receive GITR signals, as APC. Expectedly, addition of the agonistic anti-GITR mAb markedly suppressed the proliferation of iNKT cells from both liver and spleen (Fig. 2C and D, data not shown). Cytokine production by iNKT cells was also reduced by the anti-GITR mAb treatment, as show in Fig. 2E. These results strongly support the idea that GITR signals negatively regulate iNKT cell activation upon Ag stimulation.

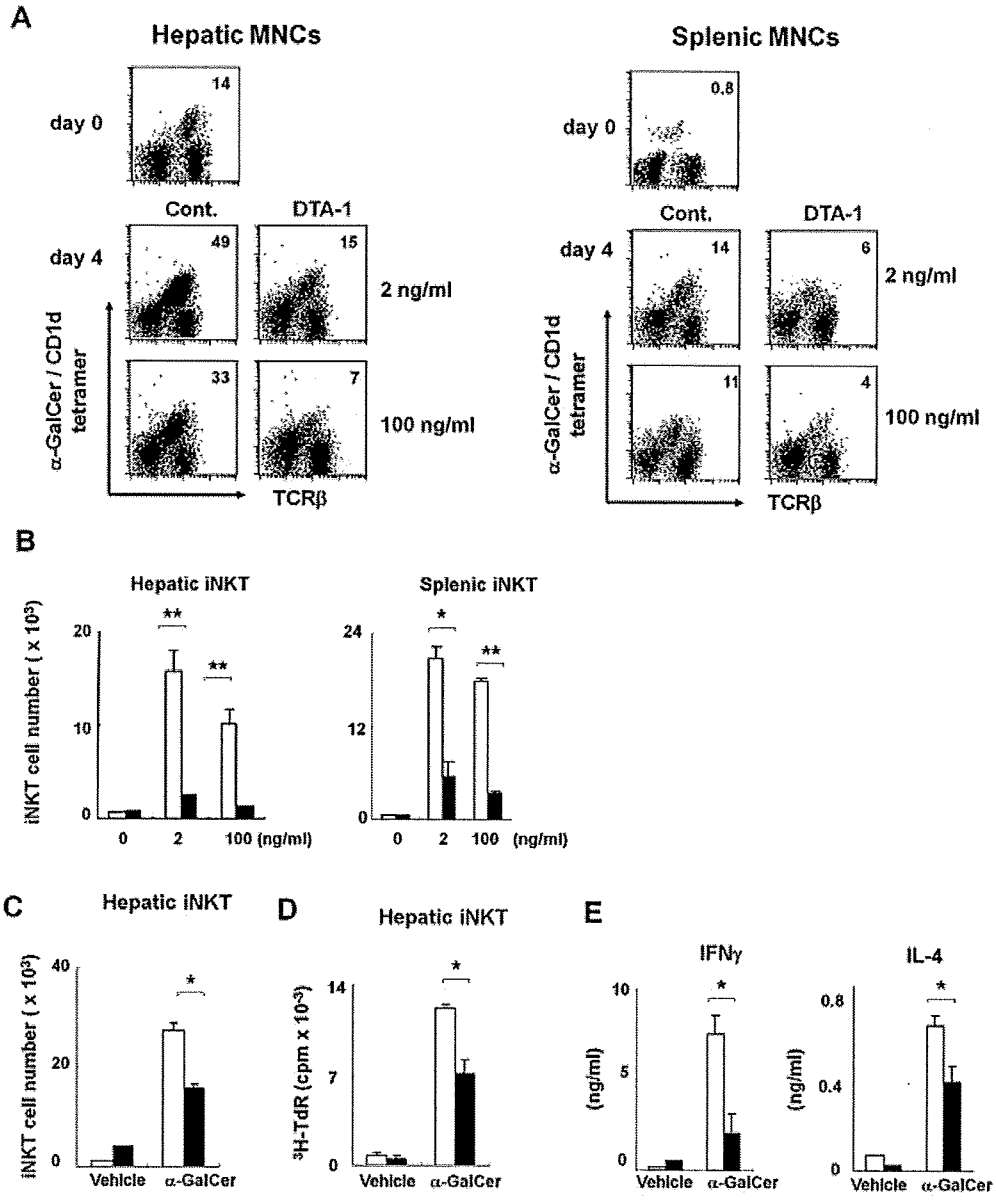

Figure 2. Agonistic anti-GITR mAb (DTA-1) inhibits α-GalCer-induced proliferation of iNKT cells, regardless of Ag dose and tissue origin. (A, B) MNC from the liver (5×10^6) (A) and spleen (2×10^5) (B) of WT mice were stimulated with higher dose (100 ng/mL) or lower dose (2 ng/mL) of α-GalCer in a 96-well round-bottom plate. Agonistic anti-GITR mAb (DTA-1; 10 μg/mL, ■) or control mAb (10 μg/mL, □) were added into the cell culture. At 4 days after stimulation, cells were stained with FITC-conjugated TCRβ and PE-conjugated α-GalCer/CD1d-tetramer and subjected to flow cytometry. (A) The frequency of TCRβ$^+$ α-GalCer/CD1d-tetramer$^+$ iNKT cells in the culture is shown. The results are representative of three mice in each genotypic group. (B) The numbers of TCRβ$^+$ α-GalCer/CD1d-tetramer$^+$ iNKT cells in the culture were counted. Results are expressed as the mean (± SD) of triplicate cultures. $^*p<0.05$, $^{**}p<0.01$. Similar results were obtained in five independent experiments. (C–E) Purified hepatic iNKT cells (1×10^5) were stimulated with 2 ng/mL α-GalCer in the presence of GITR-KO DC (1×10^5), which are unable to receive any GITR signals, in a 96-well round-bottom plate. Anti-GITR mAb (DTA-1, 10 μg/mL, ■) or control mAb (10 μg/mL, □) were added into the cell culture. (C) At 48 h after α-GalCer stimulation, the numbers of TCRβ$^+$ α-GalCer/CD1d-tetramer$^+$ iNKT cells in the culture were counted. Results are expressed as the mean (± SD) of triplicate cultures. (D) [^{3}H]Thymidine incorporation during the last 4 h of the 96-h culture was measured and expressed as the mean (± SD) of triplicate cultures. $^*p<0.05$. Similar results were obtained in three independent experiments. (E) The cell culture supernatants were collected 36 h after stimulation, and the cytokine levels in the supernatants were assayed for IFN-γ and IL-4. Results are expressed as the mean (± SD) of triplicate cultures. $^*p<0.05$, $^{**}p<0.01$. Similar results were obtained in two independent experiments.

GITR signals during Ag priming are critical for the inhibition of iNKT cell activation

We next asked whether stimulation of the GITR during Ag priming was sufficient for the GITR-mediated suppression of iNKT cell function, or whether sustained stimulation was required. To address this question, iNKT cells purified from the spleen of WT mice were stimulated with α-GalCer in the presence of GITR-KO DC for only the initial 24 h of culture, and then the number of live α-GalCer/CD1d-tetramer$^+$ TCRβ$^+$ iNKT cells was measured on the indicated days post stimulation. To provide GITR signals, the agonistic anti-GITR mAb was added for the initial 24 h, for the last 3 days, or for all 4 days. As shown in Fig. 3A and B, the engagement of GITR on iNKT cells during the initial 24 h (Ag-priming phase) significantly diminished the proliferation of iNKT cells, while the addition of anti-GITR mAb for the last 3 days, after the Ag was removed, had a negligible suppressive effect on iNKT cell proliferation. Therefore, GITR signals in iNKT cells during the Ag-priming phase are essential and sufficient for the suppression of iNKT cell activation.

Normal development of iNKT cells in GITR-deficient mice

To address the role of GITR in iNKT cell development, we next compared the frequency and absolute number of iNKT cells in the thymus, spleen, and liver between GITR-KO and WT mice. The percentage of α-GalCer/CD1d-tetramer$^+$ TCRβ$^+$ iNKT cells in these tissues was comparable in the WT and GITR-KO mice (Fig. 4A). The number of iNKT cells in the GITR-KO mice was not significantly different from that in WT mice (Fig. 4B). Further-

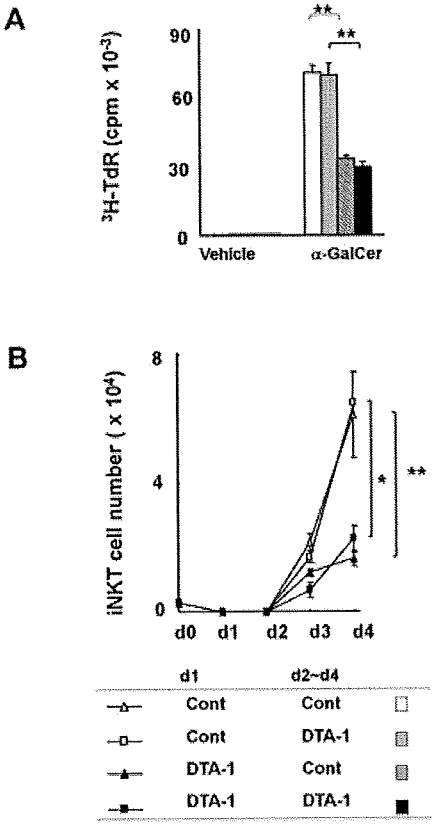

Figure 3. GITR signals during Ag priming are critical for the inhibition of iNKT cell activation. Purified WT iNKT cells (2 × 10^3) were α-GalCer-stimulated with GITR-KO DC (4 × 10^4) in the presence or absence of agonistic anti-GITR mAb as described in Fig. 2C. After 24 h of stimulation, the cells were washed and then cultured for an additional 3 days in the absence of α-GalCer. The agonistic anti-GITR mAb (DTA-1, 10 μg/mL) or control mAb (10 μg/mL) was added to the culture for the indicated days. (A) [^{3}H]Thymidine incorporation during the last 4 h of the 96-h culture was measured and expressed as the mean (± SD) of triplicate cultures. **p<0.01. (B) The numbers of live iNKT cells at the indicated days in the cell culture are demonstrated. Results are expressed as the mean (± SD) of triplicate cultures. *p<0.05, **p<0.01.

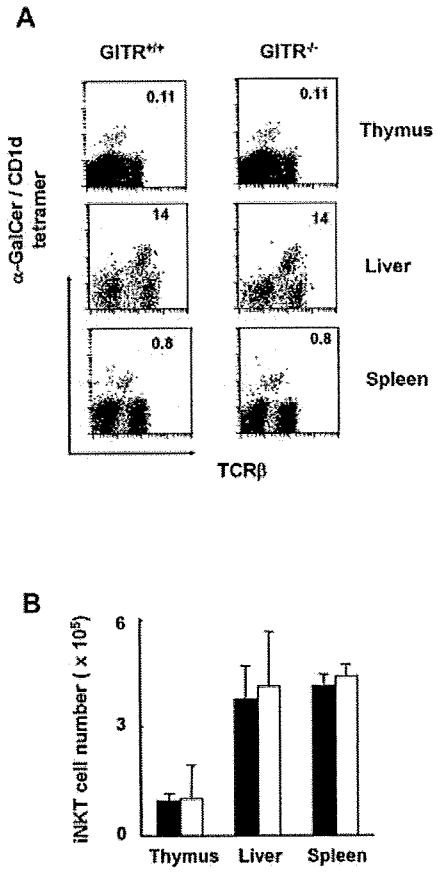

Figure 4. Normal development of iNKT cells in GITR-deficient mice. MNC isolated from the thymus, liver, and spleen of GITR-KO or WT mice were counted for cell numbers. The cells were stained with FITC-conjugated TCRβ, PE-conjugated α-GalCer/CD1d-tetramer and subjected to flow cytometry. (A) The frequency of the TCRβ$^+$ α-GalCer/CD1d-tetramer$^+$ iNKT cells in each tissue is shown. The results are representative of three mice in each genotypic group. (B) The numbers of TCRβ$^+$ α-GalCer/CD1d-tetramer$^+$ iNKT cells in the indicated tissues of GITR-KO (n=3, □) and WT (n=3, ■) mice were calculated from their frequency in MNC. Results are expressed as the mean (± SD).

more, the expression levels of iNKT-associated markers, such as CD4, CD69, Ly49A, and NKG2D, were similar between the GITR-KO and WT mice (data not shown). Collectively, these results show that, in spite of the significant expression of GITR on iNKT cells, GITR is dispensable for iNKT cell development.

GITR-KO iNKT cells show enhanced activation in response to Ag *in vitro*

We next examined *in vitro* proliferative response of α-GalCer/CD1d-tetramer$^+$ TCRβ$^+$ iNKT cells isolated from the liver of GITR-deficient mice. As shown in Fig. 5A, the recovery of GITR-KO iNKT cells after *in vitro* treatment with Ag (α-GalCer) was significantly higher than that from WT control iNKT cells. The DNA synthesis by GITR-KO iNKT cells upon Ag stimulation was also enhanced compared with that of WT controls (Fig. 5B). The culture supernatant of the purified iNKT cells from the liver of GITR-KO or WT mice was measured for IFN-γ and IL-4. Ag treatment caused a higher production of these cytokines in GITR-KO iNKT cells than in WT iNKT cells (Fig. 5C). These results are consistent with the observations using agonistic anti-GITR mAb, treatment of which suppresses the Ag-induced activation of iNKT cells.

Lack of GITR enhances iNKT cell activation *in vivo*

The *in vivo* effects of GITR signals on the Ag-induced iNKT cell activation were investigated. We injected α-GalCer i.p. into GITR-KO mice and examined the *in vivo* proliferation of α-GalCer/CD1d-tetramer$^+$ TCRβ$^+$ iNKT cells. Thymectomized mice were used to avoid the interfusion of newly differentiated naïve iNKT cells from the thymus. As expected, the number of the tetramer$^+$ iNKT cells was significantly increased in the liver and spleen of thymectomized GITR-deficient mice; the values were twice those seen in the thymectomized WT mice (Fig. 6A). Similar results were obtained when using a non-thymectomized mice combination (data not shown).

To address whether the increased number of Ag-activated iNKT cells in GITR-KO mice may be mediated by an apoptotic mechanism, we examined apoptosis of iNKT cells in the α-GalCer-treated thymectomized mice using Annexin V staining. Fig. 6B demonstrated that the intensity level for Annexin V staining after Ag stimulation between WT and GITR-KO iNKT cells were similar. Therefore, the increase in iNKT cell number seen in GITR-deficient mice is mainly mediated by cell proliferation rather than apoptosis.

We next examined cytokine secretion of GITR-KO iNKT cells during Ag-induced activation. The GITR-KO mice showed higher serum levels of IFN-γ and IL-4 upon i.p. injection with α-GalCer (Fig. 6C). *Ex vivo* intracellular cytokine staining demonstrated that Ag-stimulation induces higher production of IL-4 and IFN-γ by iNKT cells in GITR-deficient mice than in WT mice (Fig. 6D). Collectively, GITR deficiency promotes not only proliferation but also cytokine production of iNKT cells upon *in vivo* stimulation with α-GalCer.

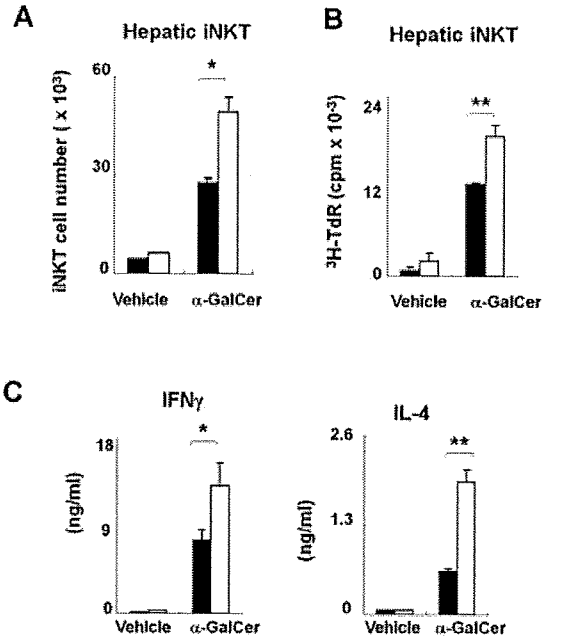

Figure 5. GITR-deficient iNKT cells show enhanced activation in response to Ag in *vitro*. Purified α-GalCer/CD1d-tetramer$^+$ iNKT cells from the liver of GITR-KO (□) or WT mice (■) were stimulated with α-GalCer (2 ng/mL) in the presence of GITR-KO DC as described in Fig. 2C. (A) The numbers of live iNKT cells 48 h after stimulation are demonstrated. Results are expressed as the mean (± SD) of triplicate cultures. $^*p<0.05$. (B) [^{3}H]Thymidine incorporation during the last 4 h of the 48-h culture was measured as an indicator of cell proliferation and expressed as the mean (± SD) of triplicate cultures. $^*p<0.05$, $^{**}p<0.01$. Similar results were obtained in two independent experiments. (C) The cell culture supernatants were collected 36 h after stimulation, and the cytokine levels in the supernatants were assayed for IFN-γ and IL-4. Results are expressed as the mean (± SD) of triplicate cultures. $^*p<0.05$, $^{**}p<0.01$. Similar results were obtained in two independent experiments.

Lack of GITR enhances iNKT cell-mediated anti-tumor immunity

Finally, to evaluate the *in vivo* roles for GITR, we set up an *in vivo* experimental system in which iNKT cells mediate anti-tumor immunity. The *ex vivo* cytotoxic activity of hepatic MNC derived from α-GalCer-treated GITR-KO mice on EL-4 cells was significantly higher than that of hepatic MNC from α-GalCer-treated WT mice (Fig. 7A). EL-4 cells were injected i.v. and 600 ng α-GalCer or vehicle was injected i.p. into WT or GITR-deficient mice. Although both the WT and GITR-KO mice died from liver metastasis of the tumor cells by 14 days after tumor injection when vehicle alone was administered, all of the α-GalCer-treated mice were alive at 14 days (Fig. 7B). However, the prolonged survival of the α-GalCer-treated WT mice (median survival = 17 days) compared with that of the vehicle-treated mice (median survival = 14 days) did not reach statistical significance, probably because our experimental protocol used a dose of α-GalCer that was about tenfold less than the usual dosage for enhancing anti-tumor

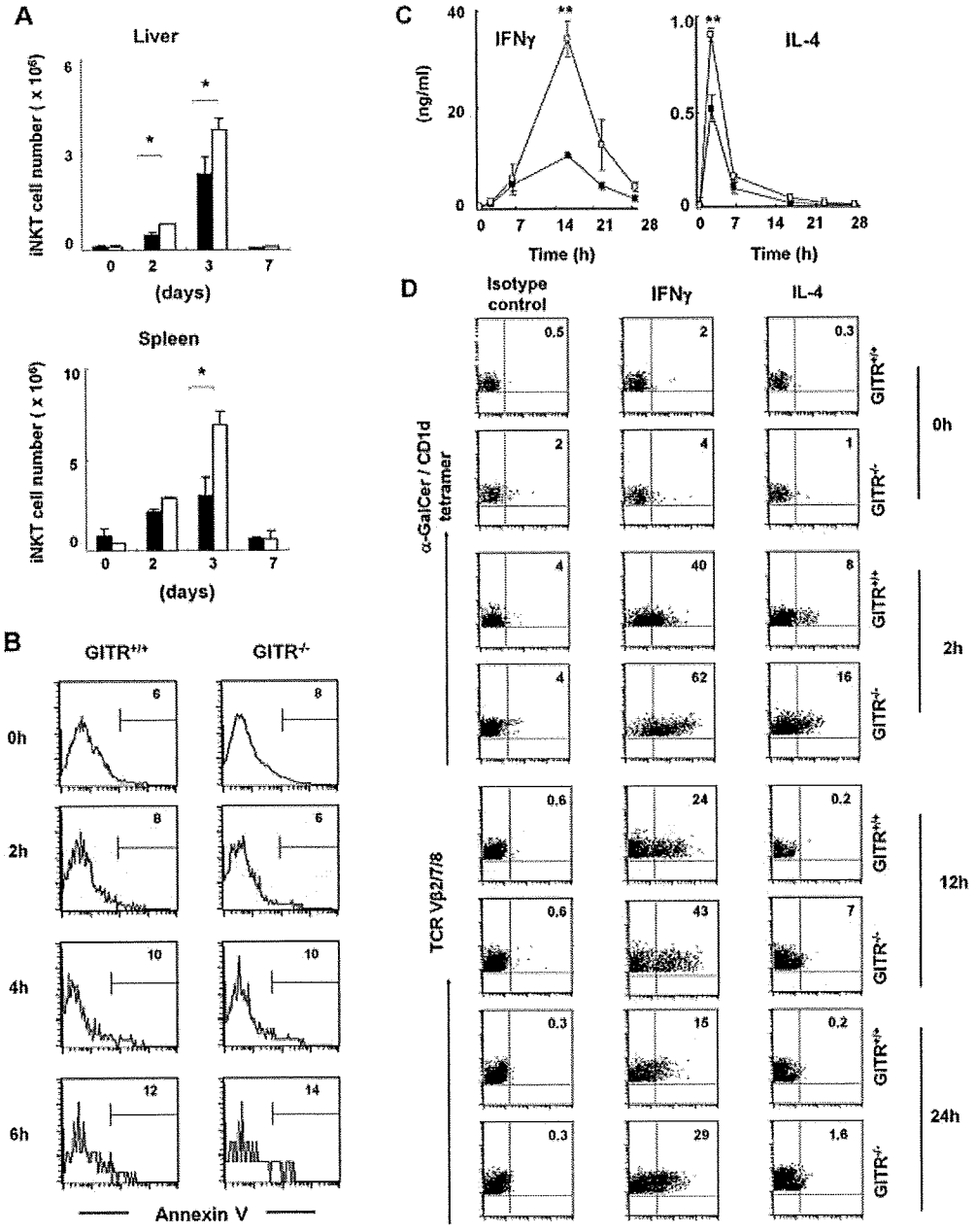

Figure 6. Lack of GITR promotes *in vivo* proliferation and cytokine production of iNKT cells. (A, B) Thymectomized GITR-KO (n=3, □) and WT (n=3, ■) mice were i.p. injected with 2 μg α-GalCer. (A) On days 2, 3 and 7 after injection, the absolute number of TCRβ$^+$ α-GalCer/CD1d-tetramer$^+$ iNKT cells in the liver and spleen of each mice are demonstrated. Results are expressed as the mean (± SD). *p<0.05. (B) Hepatic MNC were isolated from the thymectomized GITR-KO and WT mice at the indicated time after α-GalCer injection, and stained with allophycocyanin-conjugated Annexin V. The staining of electrically gated α-GalCer/CD1d-tetramer$^+$ TCRβ$^+$ cells in hepatic MNC is shown. The number shown in each panel represents the percentage of iNKT cells that were positive for Annexin V. (C, D) GITR-KO (n=3, □) and WT (n=3, ■) mice were i.p. injected with 2 μg α-GalCer. (C) Serum was collected at the indicated time for the cytokine measurement (IFN-γ and IL-4) by ELISA. Similar results were obtained in two independent experiments. (D) At 2, 12 and 24 h after α-GalCer stimulation, hepatic MNC were isolated, and cultured in the presence of Brefeldin A for 2 h without further stimulation. Intracellular staining of IFN-γ and IL-4 in α-GalCer /CDd tetramer$^+$ cells (0 and 2 h) and in TCR Vβ2/7/8$^+$ cells (12 and 24 h) was carried out. The number shown in each panel represents the percentage of iNKT cells that were positive for intracellular IFN-γ or IL-4. Similar results were obtained in three independent experiments.

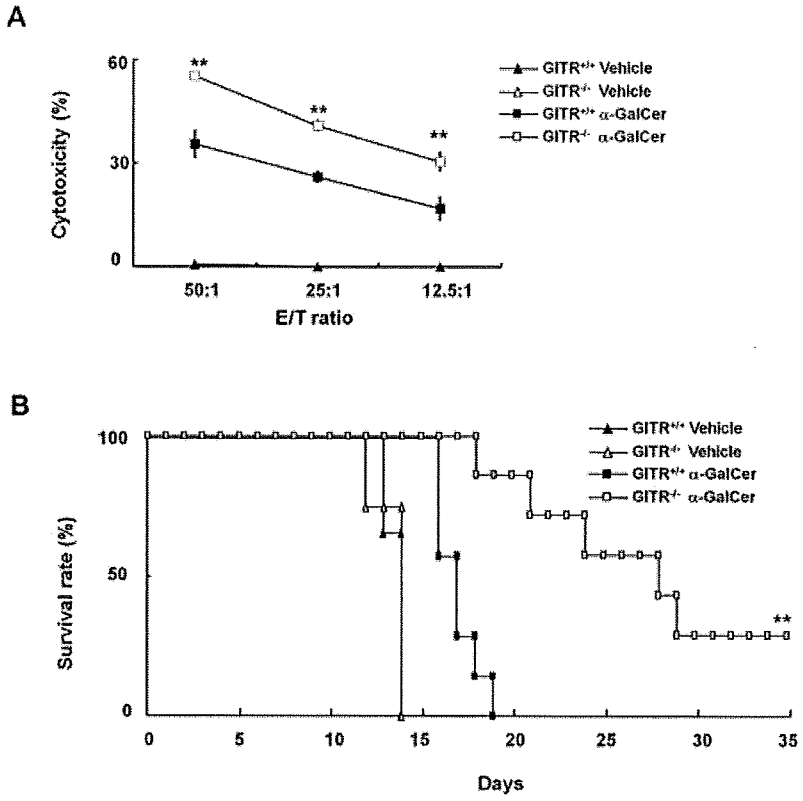

Figure 7. Lack of GITR promotes α-GalCer-mediated anti-tumor immunity. (A) Hepatic MNC were isolated from GITR-KO (□, △) and WT mice (n=3, ■, ▲) 24 h after the i.p. injection of α-GalCer (2 μg; □, ■) or vehicle (△, ▲), and incubated with ^{51}Cr-labeled EL-4 cells for 4 h. Radioactivities of the supernatants were determined with a γ-counter. Data shown are representative of three experiments. Results are expressed as the mean ± SD. *p<0.05. (B) EL-4 cells were injected i.v. into each mouse. On the same day, 600 ng α-GalCer (□, ■) or the same volume of vehicle (△, ▲) was injected i.p. The survival time of each mouse (n=7 in each group) was recorded. GITR-KO mice treated with α-GalCer (□) had significantly delayed mortality compared with α-GalCer-treated WT mice (■; log-rank **p<0.005).

immunity. In spite of the low α-GalCer dose, the α-GalCer was very effective in promoting the survival of the GITR-KO mice (median survival = 28 days, log-rank p<0.005). Taken together, these results indicate that GITR signals suppress the *in vivo* cytotoxic activity of iNKT cells for tumor cells.

Discussion

The present results suggest that signals through GITR can function as a negative regulator on iNKT cell activation in contrast to the positive roles of other costimulatory molecules including CD28, ICOS, CD40, and OX40 [15–17, 19, 22]. In addition, in spite of the down-regulation of TCR, NK cell receptors, and costimulatory molecules on the surface of recently activated iNKT cells, GITR expression is rather enhanced upon stimulation with α-GalCer (Fig. 1C). This suggests that recently activated iNKT cells are still ready to respond to GITR stimulation, but not to Ag or other costimulatory stimulation. The down-regulation of TCR and other costimulatory molecules might contribute to preventing over-activation of iNKT cells because CD28, ICOS and OX40 enhance iNKT cell activation [15–17, 19, 22]. The opposite function and expression profile of GITR to those of other costimulatory molecules suggest that GITR signals might play a role in counteracting the activation of iNKT cells to maintain homeostasis of iNKT cells.

GITR most closely resembles OX40 in the protein and gene structures and in immunological roles [6, 7, 27–32]. In addition, the genomes for OX40 and GITR might be evolutionarily derived from one gene because these genes are contiguously located on the same chromosomal locus, suggesting the redundant roles between OX40 and GITR. However, the effect of GITR signals in iNKT cells seems opposite to that of OX40. This conclusion may be supported by our preliminary results using GITR-OX40L-double KO mice. α-GalCer-induced iNKT cell proliferation and cytokine production in GITR-OX40L-double KO mice were reduced as compared with those in GITR-KO mice, but were much higher than those in OX40L-KO mice (our unpublished data). These results suggest that GITR and OX40 signals might be mutually nonredundant in iNKT cell function.

With regard to the suppressive functions of GITR in T cells, several findings have been reported. Tone *et al.* [9] have

demonstrated that GITR signals in the presence of high-dose Ag suppress T cell proliferation, while these signals in the presence of low-dose Ag promote the proliferation. Thus, we examined whether the effect of GITR signals differed in the presence of different Ag doses. In contrast to the case for T cells, similar suppressive effects by GITR were seen regardless of the Ag dose (Fig. 2, and data not shown). Although Tone *et al.* [9] suggest that *in vitro* GITR signals along with high-dose Ag may induce T cell apoptosis, which may lead to reduced T cell proliferation, we could not observe any difference in apoptosis between GITR-KO iNKT and WT iNKT cells after Ag stimulation (Fig. 6B). Thus, the mechanisms for the suppressive effects by GITR signals on T and iNKT cells might be different. On the other hand, a recent paper suggests that GITRL signals in DC induce suppressive immune responses through T cell and DC interaction. Since we used DC as APC *in vitro* cultures, signals through GITRL in DC might also contribute to the inhibition of iNKT cell function. To understand the mechanisms for the suppressive roles of GITR, further experimental evidence will be required.

One previous paper demonstrated that the engagement of GITR on NKT cell hybridomas and NK1.1$^+$ TCRβ$^+$ cells using agonistic anti-GITR mAb enhanced the cytokine production by these cells during activation [23]. These results appear to be the opposite of ours. However, Kim *et al.* [23] used the co-expression of NK1.1 and TCRβ as a marker for NKT cells. As mentioned in the introduction section, NK1.1$^+$ TCRβ$^+$ NKT cells may be a little different from α-GalCer/CD1d-tetramer$^+$ TCRβ$^+$ iNKT cells [3, 24], although some of these populations may overlap. Furthermore, the NK1.1$^+$ TCRβ$^+$ cells used in the previous study were stimulated with an anti-CD3 mAb instead of α-GalCer in most experiments [23]. Indeed, we failed to produce significant cell proliferation of α-GalCer/CD1d-tetramer$^+$ TCRβ$^+$ iNKT cells when anti-CD3 mAb was used according to the experimental procedure of Kim *et al.* (data not shown). In these contexts, the different results might be due to the difference in the NKT cell population used, and perhaps in the cell stimulation conditions. Nevertheless, our *in vivo* results using GITR-KO mice provide more specific evidence for GITR roles on α-GalCer/CD1d-tetramer$^+$ TCRβ$^+$ iNKT cell function.

Since the *in vivo* administration of α-GalCer or α-GalCer-treated DC effectively promotes anti-tumor immunity in mice, iNKT cells may be a promising target for anti-tumor therapies [3, 33]. Costimulatory signals through CD28, ICOS, and OX40 contribute to the cytokine production and cytotoxic activity of α-GalCer-activated iNKT cells [15–17, 19–22]. In addition, our results indicate that the lack of GITR signals enhances not only the cytokine production but also the proliferation of iNKT cells upon α-GalCer stimulation both *in vitro* and *in vivo*. Therefore, an *in vivo* blockade of GITR signals might induce the favorable anti-tumor effects mediated by iNKT cells, and could be augmented with protocols involving other stimulatory molecules, such as CD28, ICOS, and OX40. GITR might therefore be a useful target of immune therapies for cancer. In addition, several lines of evidence show the causative association of iNKT cell dysfunction with the development of autoimmune diabetes seen in NOD mice [34]. Enhancement of iNKT cell function by blocking GITR signals might also be a therapeutic strategy for autoimmune diseases in which impairment of iNKT cell function is involved. However, the deliberate engagement of GITR also leads to enhanced immune responses, such as autoimmunity and anti-tumor immunity, by breaking the regulatory T cell-mediated tolerance under certain conditions [35–40]. Therefore, the effects of GITR on immune responses may depend on the experimental conditions. Future studies will be necessary to elucidate the various roles of GITR in anti-tumor immunity.

Materials and methods

Mice

The GITR-deficient (GITR-KO) mice have been described previously [8]. WT mice were purchased from Japan SLC (Shizuoka, Japan). Age- (6–10 weeks old) and sex-matched WT mice were used as controls. All the mice were on a C57BL/6 background, and they were bred and maintained under specific-pathogen-free conditions. All procedures were performed according to the protocols approved by the Institutional Committee for Use and Care of Laboratory Animals of Tohoku University.

Cells

EL-4, a mouse T cell lymphoma line, was maintained in RPMI 1640 medium supplemented with 10% FBS, 100 U/mL penicillin, and 100 μg/mL streptomycin.

Ab and reagents

FITC-conjugated anti-TCRβ (H57–597), FITC-conjugated CD19 (1D3), PE-conjugated anti-Vβ2 TCR (B20.6), PE-conjugated anti-Vβ7 TCR (TR310), PE-conjugated anti-Vβ8 TCR (F23.1), biotin-conjugated anti-CD28 (37.51), biotin-conjugated anti-CD94 (18d3), biotin-conjugated anti-NKG2A (16a11), biotin-conjugated anti-ICOS (7E.17G9), biotin-conjugated anti-OX40 (OX86), allophycocyanin-conjugated anti-IFN-γ (XMG1.2), allophycocyanin-conjugated anti-IL-4 (11B11), and isotype control Ab were purchased from BD PharMingen (San Diego, CA). Purified, biotin- and allophycocyanin-conjugated anti-GITR mAb (DTA-1) were purchased from eBioscience (San Diego, CA). α-GalCer (KRN7000) was provided by Kirin Brewery (Gunma, Japan). Brefeldin A solution, allophycocyanin-conjugated Annexin V and 7-amino actinomycin (7AAD) were purchased from BD PharMingen.

Flow cytometry

To prevent nonspecific binding of Ab to FcRγ, cells were preincubated with anti-mouse CD16/32 (2.4G) before staining with specific Ab. Anti-TCRβ and α-GalCer/CD1d tetramer were used to detect iNKT cells as previously described [41]. In brief, cells were incubated with the indicated mAb and/or PE-conjugated α-GalCer/CD1d tetramer for 30 min at 4°C, then washed with PBS and analyzed with a FACSCalibur flow cytometer (BD Biosciences, Mountain View, CA). When using biotin-conjugated mAb, the cells were further incubated with PE- or allophycocyanin-conjugated streptavidin for 20 min. The analyses were conducted using the CellQuest program (BD Biosciences). To define iNKT cells at 24 h after α-GalCer stimulation, intracellular staining with the mixture of PE-conjugated anti-Vβ2, anti-Vβ7, and anti-Vβ8 TCR mAb was performed with a BD Cytofix/Cytoperm kit (BD Pharmingen) according to the manufacturer's instruction.

Purification of iNKT cells

Hepatic or splenic MNC were stained with FITC-conjugated anti-TCRβ and PE-conjugated α-GalCer/CD1d tetramer. The α-GalCer/CD1d-tetramer$^+$ TCRβ$^+$ cells were then sorted by a FACSAria cell sorter (BD Biosciences). The purity of the sorted cells was at least 95%.

Preparation of DC

Splenic DC were prepared as previously described [42]. In brief, the spleens of GITR-KO mice were treated with collagenase type III (400 U/mL; Sigma, St. Louis, MO) for 60 min at 37°C. The resulting single cells were incubated with CD11c MicroBeads (Miltenyi Biotec) for 15 min at 4°C. CD11c$^+$ cells were separated by an AutoMACS cell sorter (Miltenyi Biotec). The CD11c$^+$ fraction was typically ≥95% pure and used as DC (APC) for *in vitro* iNKT cell stimulation.

In vitro activation of iNKT cells

Hepatic (5×10^4) or splenic (2×10^5) MNC were stimulated with 2 ng/mL or 100 ng/mL α-GalCer for the indicated time in a 96-well round-bottom plate. Purified hepatic iNKT cells (1×10^5) were stimulated with 2 ng/mL α-GalCer in the presence of GITR-KO DC (APC; 1×10^5), which cannot receive any GITR signals. Splenic iNKT cells (2×10^3) were stimulated with 100 ng/mL α-GalCer in the presence of GITR-KO DC (4×10^4). To provide deliberate GITR signals, an agonistic anti-GITR mAb (DTA-1; 10 μg/mL) or control mAb was added to the culture. In some experiments, after 24 h of stimulation with α-GalCer, the cells were washed and cultured for an additional 3 or 4 days in the absence of α-GalCer. To measure proliferation incorporation of [^{3}H]thymidine in the cells was measured as previously described [43]. In brief, [^{3}H]thymidine (1 μCi/well) was added to 48- or 96-h cultures for the final 4 h at the time indicated. The mean incorporation of thymidine into DNA was measured as an indicator of cell proliferation and expressed as the mean (± SD) of triplicate cultures. Alternatively, cells were collected for flow cytometry at the indicated times. To detect cytokine production, the cell culture supernatants were collected 36 or 72 h after stimulation. The cytokine levels in the supernatants were assayed using ELISA kits for IFN-γ and IL-4 (BD Biosciences) according to the manufacturer's instruction.

Thymectomy

The upper part of the thoracic cavity of anesthetized mice was carefully opened to enable removal of the thymus with an aspirator. The wound was closed with surgical staples, and the mice were kept warm until fully recovered. The completeness of thymectomy was checked when the mouse was killed and those with remnants of thymus tissue were excluded from analysis. The thymectomized mice were subjected to *in vivo* experiments at least 3 weeks after thymectomy.

In vivo activation of iNKT cells

Mice were given i.p. injections of 2 μg α-GalCer. Serum was obtained at the indicated times, and the serum concentrations of IFN-γ and IL-4 were measured by ELISA. Intracellular staining of IFN-γ and IL-4 was carried out at 2, 12, and 24 h after α-GalCer injection. Briefly, MNC were isolated from the liver at the indicated time and cultured for 2 h in Brefeldin A without further stimulation. Surface labeling and intracellular staining were performed following the manufacturer's instruction (BD Cytofix/Cytoperm kit). On days 2, 3 and 7 after the α-GalCer injection, the number of live iNKT cells in the liver and spleen was calculated by counting the total cell number and frequency of α-GalCer/CD1d-tetramer$^+$ TCRβ$^+$ cells by flow cytometry. Apoptosis of iNKT cells was determined by Annexin V labeling at 2, 4, and 6 h after α-GalCer challenge. MNC were isolated from the liver at the indicated times and incubated with allophycocyanin-conjugated Annexin V in Annexin V binding buffer according to the manufacture's instruction. 7-amino actinomycin (7AAD) was added 10 min before acquisition to exclude dead cells.

Cytotoxicity assay

The cytolytic activity against NK-resistant EL-4 cells as target cells was assessed by a standard ^{51}Cr-release assay. As effector cells, hepatic MNC were collected from mice 24 h after i.p. injection with 2 μg α-GalCer. These cells were then incubated with ^{51}Cr-labeled EL-4 cells at the indicated ratios for 4 h. After the incubation, the radioactivity of the supernatants was determined with a γ-counter. The results were expressed as the % specific lysis

